JACS
JOURNAL OF THE AMERICAN CHEMICAL SOCIETY
pubs.acs.org/JACS
Article

Inhibition of Isoleucyl-tRNA Synthetase by the Hybrid Antibiotic Thiomarinol

Rachel A. Johnson,[#] Andrew N. Chan,[#] Ryan D. Ward, Caylie A. McGlade, Breanne M. Hatfield, Jason M. Peters, and Bo Li*

Cite This: *J. Am. Chem. Soc.* 2021, 143, 12003–12013
Read Online
ACCESS | Metrics & More | Article Recommendations | Supporting Information

ABSTRACT: Hybrid antibiotics are an emerging antimicrobial strategy to overcome antibiotic resistance. The natural product thiomarinol A is a hybrid of two antibiotics: holothin, a dithiolopyrrolone (DTP), and marinolic acid, a close analogue of the drug mupirocin that is used to treat methicillin-resistant *Staphylococcus aureus* (MRSA). DTPs disrupt metal homeostasis by chelating metal ions in cells, whereas mupirocin targets the essential enzyme isoleucyl-tRNA synthetase (IleRS). Thiomarinol A is over 100-fold more potent than mupirocin against mupirocin-sensitive MRSA; however, its mode of action has been unknown. We show that thiomarinol A targets IleRS. A knockdown of the IleRS-encoding gene, *ileS*, exhibited sensitivity to a synthetic analogue of thiomarinol A in a chemical genomics screen. Thiomarinol A inhibits MRSA IleRS with a picomolar K_i and binds to IleRS with low femtomolar affinity, 1600 times more tightly than mupirocin. We find that thiomarinol A remains effective against high-level mupirocin-resistant MRSA and provide evidence to support a dual mode of action for thiomarinol A that may include both IleRS inhibition and metal chelation. We demonstrate that MRSA develops resistance to thiomarinol A to a substantially lesser degree than mupirocin and the potent activity of thiomarinol A requires hybridity between DTP and mupirocin. Our findings identify a mode of action of a natural hybrid antibiotic and demonstrate the potential of hybrid antibiotics to combat antibiotic resistance.

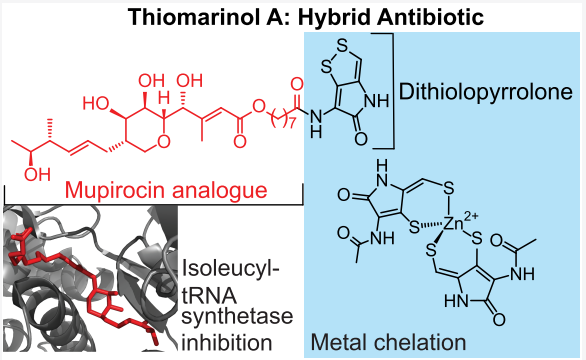

INTRODUCTION

A pressing global health concern of the 21st century is the escalating problem of antimicrobial resistance and insufficient development of the antimicrobial pipeline.[1] Natural products from plants and microorganisms harbor unique chemical structures and can exhibit potent antimicrobial activities. In fact, the majority of the antibiotics in clinical use are natural products or derivatives thereof;[2] yet, the discovery of new antimicrobial classes from both natural and synthetic sources has dwindled drastically since the 1960s. Combination therapy of antibiotics or of an antibiotic and an adjuvant can reduce or overcome antibiotic resistance, albeit formulation and administration of the combinations can require extensive optimization.[3,4] An alternative to combination treatment is covalently linking antibiotics to create a hybrid or bifunctional antibiotic; these compounds consist of two conjugated antibiotics (to achieve dual targeting) or an antibiotic linked to an adjuvant (to improve drug uptake or activity).[4] The first bifunctional antibiotic, cefiderocol, was approved for clinical use by the FDA in 2019 (Figure S1).[5] As a synthetic siderophore-β-lactam conjugate, the drug uses a "Trojan horse" mechanism, mimicking a siderophore to exploit the siderophore transport systems of Gram-negative bacteria for efficient uptake of the β-lactam antibiotic hybrid.[5] This example shows the promise of repurposing existing antibiotics through fusion to an additional chemical scaffold to broaden the antimicrobial spectrum and evade existing antibiotic resistance mechanisms.[6]

A few hybrid antibiotics have been isolated from natural sources: the simocyclinones, everninomicin P, and the thiomarinols (Figure S1). The simocyclinones consist of an aminocoumarin linked to an angucycline (Figure S1) and are over 80 times more active than derivatives lacking either component.[7,8] Unlike standalone aminocoumarins that act as competitive inhibitors for ATP in the GyrB subunit of DNA gyrase, simocyclinone prevents DNA binding through interactions with the GyrA subunit in two distinct pockets.[9] This example reveals that the mechanism of a hybrid antibiotic may differ from its constituents. A coumarin derivative is also found in the hybrid natural product, isocoumarindole A, which exhibits mild antifungal activity, but its mode of action is

Received: March 9, 2021
Published: August 3, 2021

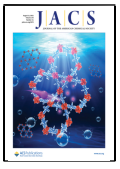

https://doi.org/10.1021/jacs.1c02622
J. Am. Chem. Soc. 2021, 143, 12003–12013

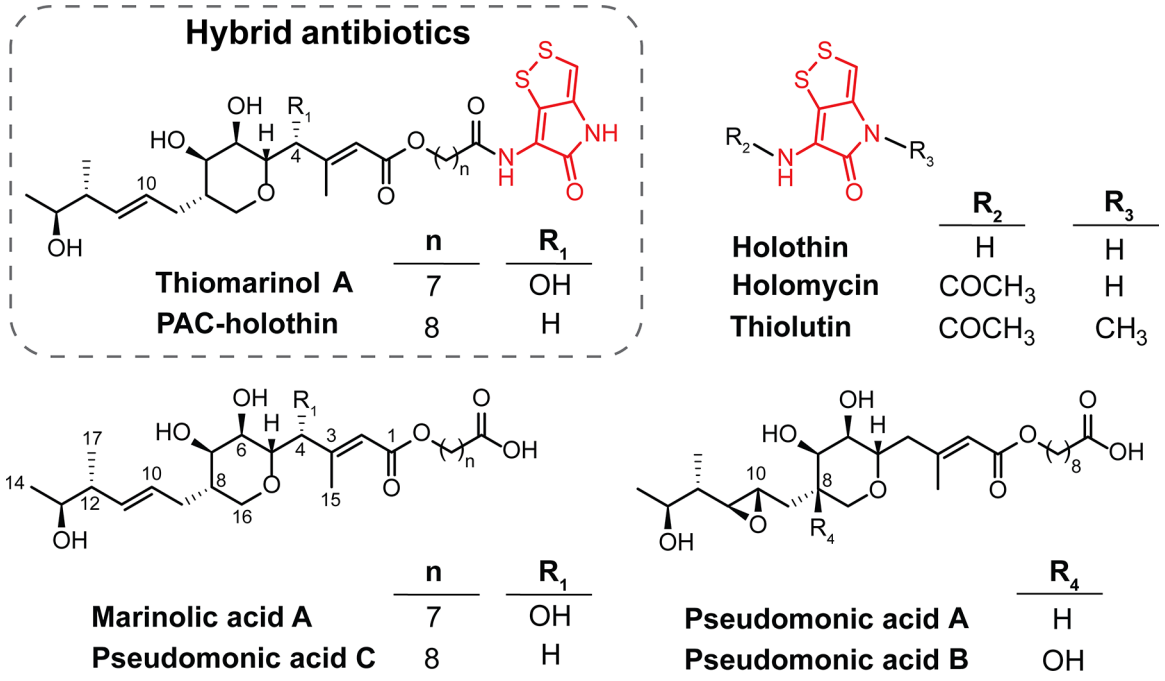

Figure 1. Structures of the antibiotics discussed in the study. Thiomarinol A is a hybrid of a dithiolopyrrolone (DTP, red) and marinolic acid, a pseudomonic acid derivative. Pseudomonic acids A, B, and C are components of the drug mupirocin. Pseudomonyl C holothinamide (PAC-holo) is a synthetic analogue of thiomarinol A. Thiomarinol, holothin, holomycin, and thiolutin are all DTP natural products.

unknown.[10] Everninomicin P is a recently discovered hybrid of the octasaccharide antibiotic everninomicin F and a glycosylated macrolide, rosamicin, linked through a unique nitrone moiety (Figure S1).[11] While it is unclear if everninomicin P is naturally produced or generated under laboratory culture conditions, the hybrid is effective against *Escherichia coli* mutants resistant to either macrolides or octasaccharides by targeting the orthogonal octasccharide- or macrolide-binding site on the 70S ribosome,[11] emphasizing the ability of hybrid antibiotics to overcome resistance.

The thiomarinols were first identified from *Pseudoalteromonas* sp. SANK 73390 (thiomarinol A–G, Figure S1) in 1993.[12−14] The major species, thiomarinol A, consists of a dithiolopyrrolone (DTP), holothin, and a polyketide, marinolic acid A (Figure 1).[12] DTPs, including holothin, holomycin, and thiolutin, are a class of broad-spectrum antimicrobial natural products that contain a characteristic bicyclic ene-disulfide moiety (Figure 1).[15−17] DTPs exert a unique mode of action as intracellular metal chelators upon cytoplasmic reduction.[18] Reduced DTPs can sequester both labile and enzyme-bound metal ions, particularly zinc, which leads to dysregulation of metal homeostasis and inhibition of metalloenzymes responsible for essential bacterial processes, such as respiration and glycolysis.[18] Thiolutin, the *N*-methyl analogue of holomycin, inhibits several Zn-dependent proteases including Rpn11 in the 26S proteasome, a promising anticancer target.[19] Inhibition of these proteases was also observed for a panel of DTPs including thiomarinol and its synthetic analogue pseudomonyl C holothinamide (PAC-holo, Figure 1).[19] Thus, intracellular metal chelation represents a central mechanism for the antimicrobial and anticancer activities of DTPs.

The second component of thiomarinol A, marinolic acid A, is a close analogue of the pseudomonic acids that compose the antibiotic mupirocin (Figure 1). Mupirocin has been widely used to treat topical infections caused by methicillin-resistant *Staphylococcus aureus* (MRSA),[20] a World Health Organization high-priority pathogen[1] that is responsible for approximately 30% of deaths from antibiotic-resistant infections in the United States.[21] Isolated from *Pseudomonas fluorescens* NCIMB 10586 as a mixture of pseudomonic acids A, B, and C (PAA, PAB, and PAC, respectively; Figure 1), mupirocin and PAA are often referenced interchangeably since PAA is the major species (>90% w/w).[22,23] All pseudomonic acids contain a monic acid moiety linked to an octanoic acid. PAA and PAC differ in structure at C-10 by either an epoxide or an alkene, respectively, and are equally effective against various *S. aureus* strains when tested individually.[24] PAB contains an additional hydroxyl at C-8 (R_4) and is 16–32-fold less effective than PAA or PAC (minimal inhibitory concentrations (MICs) of 4 μM vs 0.25 μM against *S. aureus* Newman).[24] PAC is most similar in structure to marinolic acid A, which also contains the C-10 alkene and lacks the hydroxyl at C-8.

Mupirocin binds and inhibits the essential enzyme isoleucyl-tRNA (tRNA) synthetase (IleRS), including prokaryotic paralogues from both Gram-positive MRSA and Gram-negative *E. coli in vitro*.[25−28] IleRS is a class I aminoacyl-tRNA synthetase (aaRS) that activates L-Ile as an aminoacyl-adenylate and couples the activated L-Ile with its cognate tRNA for protein synthesis.[29,30] Bacterial aaRSs exhibit significant structural differences compared to their human counterparts,[31] which enable selective antibiotic targeting; for example, mupirocin is 8000-fold more selective for prokaryotic IleRS over mammalian IleRS.[32,33] Thus, prokaryotic aaRSs are explored as antibiotic targets in drug discovery efforts. In fact, nine different bacterial aaRSs are targeted by over a dozen natural products,[29,34] including the IleRS inhibitors SB-203207 and furanomycin (Figure S2); however, these compounds suffer from low specificity and high toxicity. Mupirocin remains the only aaRS inhibitor used to treat human infections, albeit for topical use only due to low bioavailability.[20] Crystal

https://doi.org/10.1021/jacs.1c02622
J. Am. Chem. Soc. 2021, 143, 12003−12013

Table 1. Minimal Inhibitory Concentrations (MICs) of Selected Antibiotics against Mupirocin-Susceptible and -Resistant MRSA Strains

MRSA strain	protein variant	minimal inhibitory concentration (μM)		
		mupirocin	thiomarinol A	holomycin
COL	IleRS	0.25	0.002	2.5
^{LL}MR COL	$IleRS_{V588F/V631F}$	100	0.08	2.5
	$IleRS_{F587V/V631F}$	100	0.04	2.5
	$IleRS_{V588F}$	100	0.04	5.0
^{HL}MR BAA-1556	MupA	>8000	0.50	5.0
thiomarinol-resistant COL	$IleRS_{G593D}$	3.13	0.02	5.0
	$IleRS_{P606S}$	6.25	0.01	5.0

structures of mupirocin complexed to either MRSA or *Thermus thermophilus* IleRS revealed that mupirocin occupies the binding site of the isoleucyl-adenylate reaction intermediate.[35,36] Mupirocin is a slow, tight-binding inhibitor that forms an initial enzyme−inhibitor complex with IleRS that converts into a stable complex with much higher binding affinity.[28] The inhibitory mechanism of mupirocin formed the basis for rational design efforts that yielded femtomolar inhibitors of IleRS by linking L-Ile and the monate core of mupirocin via a sulfamate to mimic the isoleucyl-adenylate intermediate.[27]

Rising clinical resistance to mupirocin is observed in MRSA strains, including both low-level (^{LL}MR) and high-level mupirocin resistance (^{HL}MR), with minimal inhibitory concentrations (MICs) in the range 16−512 μM and greater than 1024 μM, respectively.[37,38] ^{LL}MR most commonly arises from spontaneous mutations in the mupirocin binding site of the native IleRS,[37,38] whereas ^{HL}MR results from the acquisition of a plasmid containing a mupirocin-resistant, eukaryotic-like IleRS variant, MupA or MupB (Figure S3).[39−41] Although less frequently observed, the ^{HL}MR MRSA isolates are of critical concern medicinally because they render mupirocin treatments ineffective.[42]

The hybrid antibiotic thiomarinol A has been reported to be significantly more potent than mupirocin against MRSA *in vitro*.[12−14] Thiomarinol A also exhibits a broader antimicrobial spectrum that includes multiple Gram-negative bacteria, such as *E. coli* and ESKAPE pathogens *Pseudomonas aeruginosa* and *Enterobacter* spp., against which mupirocin is ineffective.[12] In addition, preliminary studies indicate that thiomarinol can inhibit MRSA expressing the ^{HL}MR IleRS variant, MupA.[43] The potent and broad-spectrum activity of thiomarinol against antibiotic-resistant pathogens showcases the therapeutic potential of this hybrid antibiotic. Despite the discovery of the thiomarinols almost three decades ago, the mode of action had not been elucidated. We aimed to investigate the mode of action of thiomarinol and discern the contribution of each constituent to the efficacy of the hybrid antibiotic.

RESULTS

To identify the mode of action of the hybrid antibiotic, we set out to investigate thiomarinol activity in comparison to mupirocin and holomycin, respective analogues of the marinolic acid and holothin constituents of thiomarinol. We extracted and purified thiomarinol A (Figure 1, hereafter thiomarinol) from *Pseudoalteromonas luteoviolacea* 2ta16 with slight modifications to previous methods.[44,45] The thiomarinol gene cluster in *P. luteoviolacea* 2ta16 shares 81% sequence identity with the original producer, *Pseudoalteromonas* sp. SANK 73390 (Figure S4).[46] The structure and purity of thiomarinol were characterized by NMR and liquid chromatography coupled with high-resolution mass spectrometry (Figures S5−S7).[45] Due to the instability of holothin, we synthesized holomycin, the stable prototypical DTP with an exocyclic *N*-acetyl group. We also generated a synthetic analogue of thiomarinol: pseudomonyl C holothinamide (PAC-holo), a hybrid of holothin and pseudomonic acid C (PAC), the pseudomonic acid whose structure is most similar to marinolic acid A (Figure 1, Figures S8−S11).[47] Compared with thiomarinol, PAC-holo contains an extra methylene in the linker region and lacks a hydroxyl group at C-4 (R_1 group). Both thiomarinol and PAC-holo display potent inhibitory activities against hospital-associated methicillin-resistant *S. aureus* (MRSA) COL with MICs of 0.002 μM, over 125-fold more potent than mupirocin or PAC (MICs of 0.25 and 0.52 μM, respectively) and 1250 times more potent than holomycin (MIC of 2.5 μM, Table 1). We also quantified the cytotoxicities of thiomarinol and holomycin against the HEK293T human cell line (EC_{50} of 3.0 ± 0.3 μM, Figure S12). The cytotoxic concentration is 3 orders of magnitude higher than the MIC for thiomarinol against MRSA.

We performed a chemical genomics screen comparing the effects of PAC-holo, mupirocin, and holomycin on essential cellular processes (Figure 2, Figure S13, and Data Sets 1 and 2). Since antibiotics generally target essential processes,[3,48] we used a CRISPR interference (CRISPRi) knockdown library that targets 94% (242/257) of essential genes in *Bacillus subtilis* 168, a model bacterium for Gram-positive bacteria.[49] Of the 257 essential *B. subtilis* genes, 91% have orthologues within *S. aureus* and 77% are also essential in *S. aureus* (Figure S14);[50] thus, hits from the *B. subtilis* chemical genomics screen can be further explored in MRSA. The *B. subtilis* library contains strains with chromosomally integrated CRISPRi machinery that reduces target gene expression by ∼3-fold; the reduced expression does not substantially perturb bacterial growth, yet it leads to partial depletion of essential gene products to allow identification of chemical−gene interactions.[49] Using PAC-holo, mupirocin, holomycin, thiolutin, and gliotoxin, a fungal toxin that also contains a redox-active disulfide,[51] we screened the *B. subtilis* CRISPRi library along with 31 other growth perturbing chemicals that have published chemical−gene interactions[49] for a total of 36 unique chemical conditions at variable concentrations.

To quantify chemical−gene interactions, the colony sizes of a knockdown strain across all conditions were analyzed by use of a variance bound *t*-test to generate a chemical−gene score[52] (Data Set 1). For a global analysis of each chemical−gene interaction, we used the median chemical−gene score from a range of concentrations for the same compound (Figure 2 and Data Set 2). Consistent with IleRS as the direct target of mupirocin,[25−28] we found that *ileS* was the most sensitized

https://doi.org/10.1021/jacs.1c02622
J. Am. Chem. Soc. 2021, 143, 12003−12013

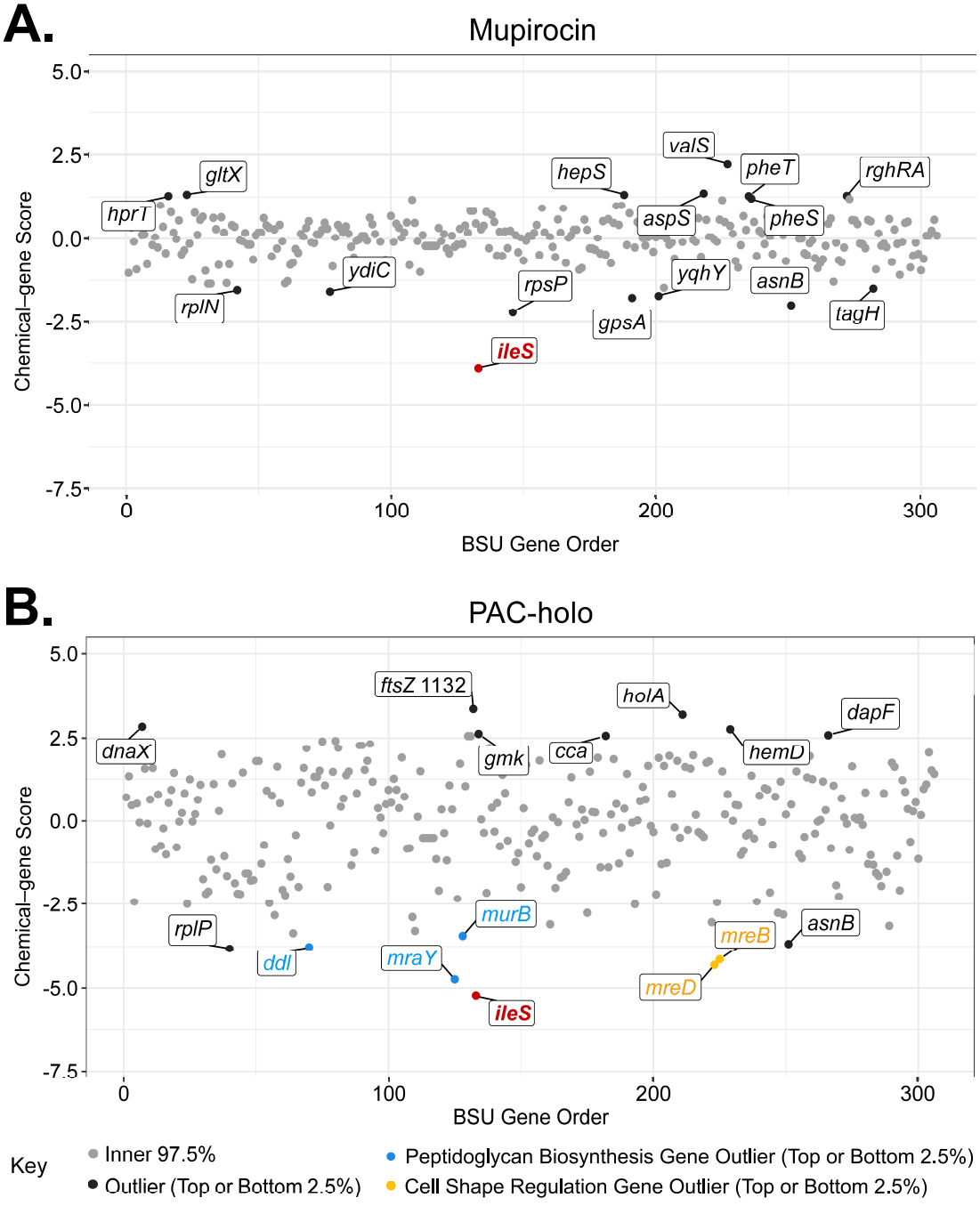

Figure 2. Hybrid antibiotic PAC-holo targets IleRS in *B. subtilis* and exerts distinctive effect from mupirocin. The knockdown of *ileS* is most sensitized in the library to treatment with (A) mupirocin or (B) PAC-holo. Genes in the top and bottom 2.5% outliers of the chemical−gene score (*y*-axis) are labeled with their gene name (*ileS* in red, genes involved in peptidoglycan biosynthesis in blue, and genes involved in cell shape regulation in yellow). Gene order (*x*-axis) corresponds to the order the genes appear in the genome of *B. subtilis*.

knockdown under mupirocin treatment (i.e., most negative chemical−gene score) (Figure 2A). We also identified *ileS* as the most sensitized knockdown under PAC-holo treatment, indicating that the hybrid antibiotic retains activity against IleRS (Figure 2B). However, other outlier strains differed between mupirocin and PAC-holo treatments (Figure 2), suggesting that the hybrid PAC-holo has distinctive effects on essential processes compared to its constituent, mupirocin. In contrast, the *ileS* knockdown was not sensitized to treatment with holomycin, thiolutin, or gliotoxin (Figure S13), hinting that these disulfide natural products do not target IleRS in cells.

We also conducted gene ontology (GO) analysis to identify cellular pathways enriched in the outlier strains of knockdowns for each antibiotic. *B. subtilis* knockdowns hypersensitive to PAC-holo are enriched in genes involved in peptidoglycan synthesis and cell shape (Figure 2B, Data Set 3). While the *ileS* knockdown is the predominant hypersensitive outlier for mupirocin, resistant outliers also include valanyl-tRNA synthetase (*valS*), aspartyl-tRNA synthetase (*aspS*), and subunits of phenylalanyl-tRNA synthetase (*pheT* and *pheS*); knockdowns of these genes might mitigate the effect of mupirocin by slowing translation. Lastly, the knockdowns hypersensitive to holomycin, thiolutin, and gliotoxin are

https://doi.org/10.1021/jacs.1c02622
J. Am. Chem. Soc. 2021, 143, 12003−12013

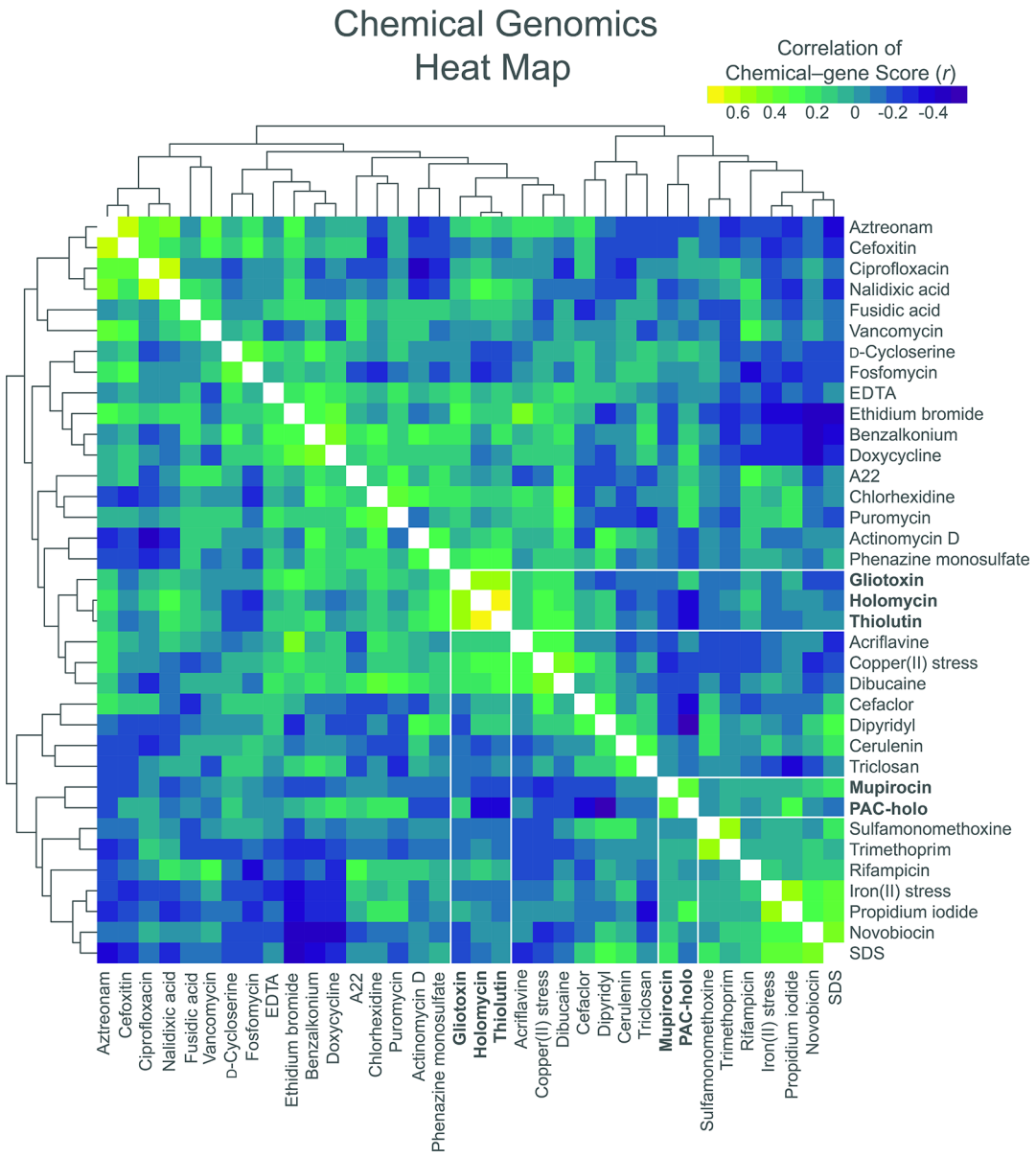

Figure 3. Chemical–gene interactions of PAC-holo correlate with mupirocin. A heat map of the Pearson correlation coefficients (r) between chemical treatments of the CRISPRi library in *B. subtilis* is shown. Higher correlation (r) of chemical–gene scores between antibiotics indicates more similar chemical–gene interactions. The range of r values is depicted with a color scale from yellow (high) to indigo (low). Self-correlations, which always have an r of 1, are shown in white, while an r of 0 denotes no correlation. Dendrograms at the top and left side of the figure show the relationship between compounds, with shorter branches indicating more similarity in chemical–gene interactions. Compounds investigated in this study are in bold.

enriched in metabolic genes, including those involved in menaquinone biosynthesis (*menA*) and cytochrome biogenesis (*resC*).

To identify broad patterns in chemical–gene interactions, we correlated chemical–gene scores across conditions and clustered the resulting matrix to group compounds that likely perturb similar essential processes (Figure 3, Data Set 3). Structurally related antibiotics cluster in this analysis, including the quinolones ciprofloxacin and nalidixic acid that inhibit DNA gyrase (r = 0.62) and the β-lactams aztreonam and cefoxitin that inhibit penicillin-binding proteins in cell wall biosynthesis (r = 0.62). Antibiotics of different structural classes that target different enzymes in the same pathway also cluster, such as the fatty acid synthesis inhibitors cerulenin and triclosan (r = 0.27), the folate synthesis inhibitors sulfamonomethoxine and trimethoprim (r = 0.53), and the cell wall biosynthesis inhibitors D-cycloserine and fosfomycin (r = 0.41).[48] Holomycin, thiolutin, and gliotoxin cluster together and exhibit the strongest correlations of all conditions in the analysis (e.g., r = 0.75 for holomycin and thiolutin), suggesting a similar mode of action for these compounds. PAC-holo clusters with mupirocin but not with holomycin or thiolutin (Figure 3), indicating that the action of PAC-holo is more similar to mupirocin than to either holomycin or thiolutin under our screening conditions; however, the correlation between PAC-holo and mupirocin is relatively modest (r = 0.37), suggesting that their modes of action do not overlap completely.

With these findings, we set out to examine IleRS as a target for PAC-holo and the natural product thiomarinol in

https://doi.org/10.1021/jacs.1c02622
J. Am. Chem. Soc. 2021, 143, 12003–12013

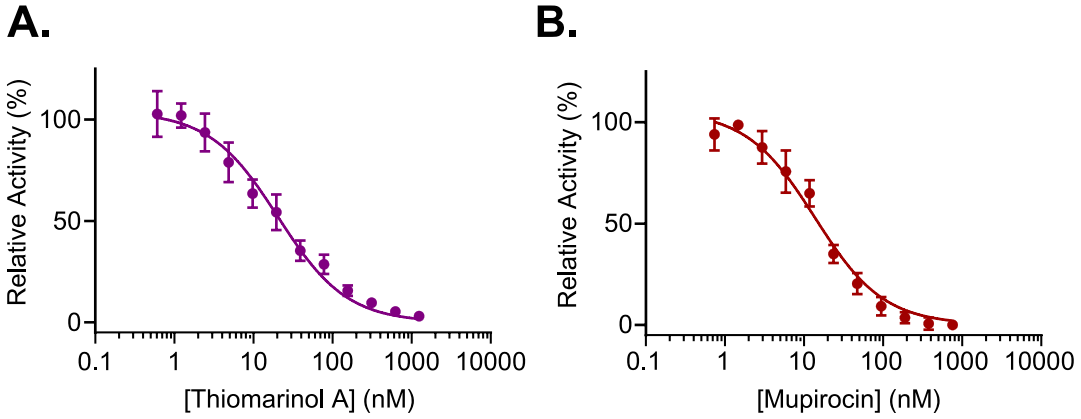

Figure 4. Thiomarinol inhibits MRSA IleRS. Dose−response curves for inhibition of 6.5 nM IleRS by (A) thiomarinol A and (B) mupirocin with K_i^{app} values of 19 ± 4 and 12 ± 2 nM, respectively. The relative adenylation activity of IleRS for L-Ile is plotted over antibiotic concentrations. Curves depict the average of four replicates for thiomarinol A and three for mupirocin. Data were fit by using the Morrison equation for tight-binding, competitive inhibitors. The inhibition constants, K_i's, were estimated to be 370 ± 70 pM for thiomarinol A and 240 ± 20 pM for mupirocin.

comparison to mupirocin using biochemical and biophysical methods. To evaluate the potency of thiomarinol against IleRS, we expressed recombinant IleRS from MRSA COL in *E. coli* (Figure S15) and measured the adenylation activity for L-Ile under steady-state conditions using an ATP-[^{32}P]-pyrophosphate (PP_i) exchange assay.[30] We conducted an active site titration of IleRS[53] that yielded 0.65 ± 0.03 active site per enzyme (Figure S16). Subsequently, we obtained an adjusted turnover number (k_{cat}) of 12.0 ± 0.5 s^{-1} and a Michaelis−Menten constant (K_M) of 40 ± 5 μM (Figure S16), which are comparable to values previously reported (k_{cat} = 18 ± 2 s^{-1} and K_M = 10 ± 2 μM).[30] With active IleRS in hand, we measured inhibition of IleRS catalysis by mupirocin, thiomarinol, and holomycin under reducing conditions. Due to the slow, tight-binding mechanism of mupirocin for IleRS, we adopted the steady-state conditions by Pope et al.[28] by preincubating the compounds with IleRS before initiating ATP-[^{32}P]PP_i exchange. The amino acid adenylation activity of IleRS was measured in the presence of increasing concentrations of each antibiotic at a saturating L-Ile concentration of 2 mM (Figure 4). Using the Morrison equation for tight-binding inhibitors,[54] we determined the apparent inhibitory constants (K_i^{app}) for mupirocin (12 ± 2 nM) and thiomarinol (19 ± 4 nM) against 6.5 nM IleRS. The K_i^{app} values of both antibiotics approach the IleRS conentration which is characteristic of tight-binding inhibitors.[54] Holomycin did not inhibit 50 nM IleRS at concentrations up to 100 μM (Figure S17). Using the K_M values for L-Ile and [L-Ile],[54] we calculated the approximate inhibitory constants (K_i) of mupirocin (240 ± 20 pM) and thiomarinol (370 ± 70 pM) for the competitive inhibition mode. Our results indicate that thiomarinol is a tight-binding inhibitor of IleRS with a potency similar to that of mupirocin.

As K_i^{app} values can be an underestimate of the potency of tight-binding inhibitors, we also quantified the binding interaction between thiomarinol and IleRS in comparison to mupirocin and holomycin. With the use of isothermal titration calorimetry (ITC), mupirocin was titrated into IleRS at room temperature (25 °C) and a 1:1 binding event was observed with an exothermic heat signature of −14.6 ± 0.4 kcal/mol (Figure S18). The reverse titration of IleRS into mupirocin yielded enthalpies ($\Delta H^{\circ\prime}$) similar to those of the forward titration (Figure S18), and these data aligned well with the reported value of −15 kcal/mol.[27] Due to the low aqueous solubility of thiomarinol, the reverse titration of IleRS into thiomarinol was performed and a single exothermic binding event was observed (Figure 5). We observed widened differential power peaks during the initial additions of IleRS into thiomarinol under reducing conditions (Figure S19); thus, we opted to perform the titration of IleRS into thiomarinol under nonreducing conditions to obtain a reliable $\Delta H^{\circ\prime}$ measurement for the binding interaction. Overall, thiomarinol−IleRS binding was less enthalpically favorable than mupirocin binding with a $\Delta H^{\circ\prime}$ of −12.4 ± 0.4 kcal/mol compared to −14.6 ± 0.4 kcal/mol (Figure 5, Figures S18 and S19, Table S1). The binding isotherms of both mupirocin and thiomarinol are step functions, indicating both antibiotics are extremely tight binders of IleRS with dissociation constants (K_d's) outside the reliable range for ITC determination.

To quantify the binding affinities of mupirocin and thiomarinol with IleRS, we used circular dichroism (CD) thermal melts as a complementary method. A change in the melting temperature (T_m) of IleRS in the presence of an antibiotic correlates to the stability of that protein−antibiotic complex. A CD scan of IleRS from 270 to 190 nm reveals a signal with local minima at ∼220 and 210 nm, representative of an α-helical secondary structure as described for IleRS;[27] this signal remains constant in the presence of different antibiotics, indicating that no detectable secondary structural changes occur in IleRS upon antibiotic binding (Figure S20). Protein ellipticity at 210 nm was measured as a function of temperature to assess IleRS stability in the presence of various antibiotics (Figure 5). The T_m of IleRS in buffer (49.0 ± 0.4 °C) agrees well with the literature value of 52 °C[27] and was not affected by the addition of holomycin (49.0 ± 0.4 °C), implying that the DTP moiety alone does not bind IleRS. The T_m of IleRS significantly increases in the presence of mupirocin, PAC-holo, or thiomarinol (Figure 5, Table S2), supporting tight binding of all three antibiotics to IleRS as an enzyme target.

We evaluated the stability of antibiotic−IleRS complex by comparing the differences in the T_m of IleRS in the presence and absence of antibiotics. The T_m's of IleRS in the presence of mupirocin and PAC-holo show no statistically significant difference, 69.3 ± 0.2 and 68.3 ± 0.6 °C respectively (Figure 5,

https://doi.org/10.1021/jacs.1c02622
J. Am. Chem. Soc. 2021, 143, 12003−12013

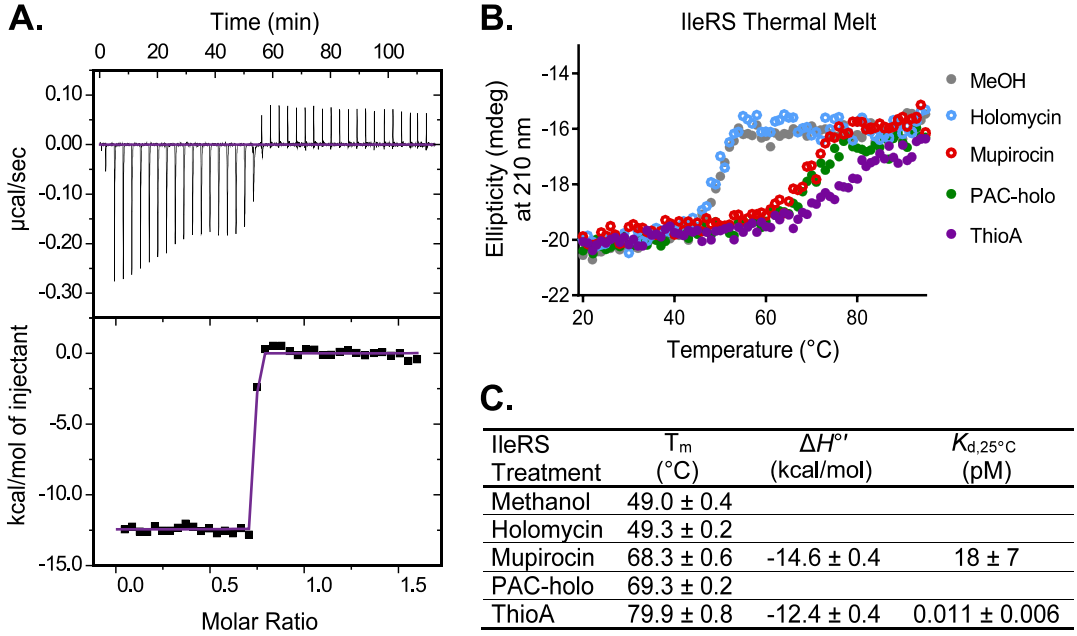

C.

IleRS Treatment	T_m (°C)	$\Delta H^{\circ\prime}$ (kcal/mol)	$K_{d,25°C}$ (pM)
Methanol	49.0 ± 0.4		
Holomycin	49.3 ± 0.2		
Mupirocin	68.3 ± 0.6	-14.6 ± 0.4	18 ± 7
PAC-holo	69.3 ± 0.2		
ThioA	79.9 ± 0.8	-12.4 ± 0.4	0.011 ± 0.006

Figure 5. Thiomarinol binds MRSA COL IleRS with high affinity. (A) Representative ITC data of 250 μM IleRS titrated into 30 μM thiomarinol A (ThioA) at 25 °C. The titration curve depicts an exothermic 1:1 binding event. (B) Representative thermal shift assay of 2.5 μM IleRS in the presence of 5 μM of each antibiotic. The CD signal, ellipticity (mdeg), of IleRS at 210 nm was measured as a function of temperature to determine the melting temperatures (T_m's). (C) Table of IleRS T_m's in the presence of each antibiotic obtained from thermal shift assay, enthalpies of binding at 25 °C, pH 7.4 ($\Delta H^{\circ\prime}$) obtained from ITC, and calculated dissociation constants ($K_{d,25\,°C}$).

Table S2). However, the T_m of IleRS binding to thiomarinol was 79.9 ± 0.8 °C, 31 °C higher than that of IleRS alone and 10 °C higher than that of IleRS in the presence of either PAC-holo or mupirocin; the substantially higher T_m suggests thiomarinol binds IleRS considerably tighter than all other antibiotics tested (Figure 5, Table S2). Additionally, IleRS maintained a similar T_m in the presence of thiomarinol or holomycin under reducing and nonreducing conditions, implying the redox state of the DTP does not affect the overall binding of thiomarinol or holomycin (Figure S21). Combining the enthalpy of binding obtained from ITC and the T_m of IleRS with and without ligands, we calculated the K_d values of mupirocin and thiomarinol binding to IleRS using derivations of the van't Hoff equation described by Brandts et al.[55] These calculations estimate that mupirocin binds IleRS at 18 ± 7 pM, while thiomarinol binds at 0.011 ± 0.006 pM, approximately 1600-fold more tightly. Thermodynamic calculations reveal that binding of both mupirocin and thiomarinol to IleRS is enthalpically driven; however, entropy contributes significantly to thiomarinol interactions with IleRS while the entropy component of mupirocin−IleRS complexation is too small to calculate (Table S1). Thus, thiomarinol forms an exceptionally tight, inhibitory complex with IleRS that is driven by both enthalpy and entropy and is estimated to bind 3 orders of magnitude tighter than mupirocin.

We measured the effectiveness of thiomarinol against both mupirocin-sensitive MRSA and mupirocin-resistant MRSA in culture. Mupirocin-sensitive MRSA COL (MIC of 0.5 μM) was subjected to increasing concentrations of mupirocin to generate mutants that exhibit low-level mupirocin resistance (^{LL}MR, MIC of 100 μM). Sequencing of *ileS* from these strains reveals spontaneous point mutations near the active site of IleRS: V588F/V631F, F587V/V631F, and V588F, among which V588F/V631F mutations are the most commonly observed ^{LL}MR genotype in clinical isolates.[56] We obtained the ATCC BAA-1556 MRSA strain that contains a mupirocin-resistant isoleucyl-tRNA synthetase, MupA,[57] and confirmed it to exhibit high-level mupirocin resistance (^{HL}MR, MIC of >8000 μM). The MICs of thiomarinol and holomycin were measured against mupirocin-sensitive MRSA COL, ^{LL}MR mutants of MRSA COL, and the ^{HL}MR strain BAA-1556. Thiomarinol retains activity against both ^{LL}MR MRSA and ^{HL}MR MRSA, although its MIC increases from 0.002 μM to 0.08 (^{LL}MR) and 0.5 μM (^{HL}MR) as the mupirocin resistance of MRSA increases (Table 1). In contrast, the MICs of holomycin remain constant at 2.5−5.0 μM against MRSA COL and both ^{LL}MR and ^{HL}MR MRSA strains, supporting that holomycin does not target IleRS.

Given that both DTP-containing molecules remain effective against MupA-containing ^{HL}MR MRSA, against which mupirocin is inactive, we proposed thiomarinol may enact additional modes of action against MRSA that are similar to other DTPs. Thus, we measured the ability of thiomarinol to chelate zinc ions. UV-vis analysis showed formation of a new thiomarinol−zinc species at 373 nm (pH 7.4) under reducing conditions (Figure S22), indicating that thiomarinol chelates zinc *in vitro*. To assess the effect of thiomarinol on metal availability in bacterial cells, we obtained the MRSA Newman mutant Δ*adcA*Δ*cntA* that is defective in zinc import and measured cell growth with and without zinc at subinhibitory concentrations of thiomarinol and holomycin (Figure S23). As reported by Grim et al., the Δ*adcA*Δ*cntA* mutant grows slower under zinc-deficient conditions than wild type (WT) MRSA ($p < 0.01$).[58] In the absence of zinc, treatment of Δ*adcA*Δ*cntA* with either thiomarinol or holomycin leads to a significant growth defect in comparison to the antibiotic-free control ($p < 0.001$). The addition of zinc restores the growth of the Δ*adcA*Δ*cntA* strain in the presence of antibiotics to WT levels, suggesting that both thiomarinol and holomycin affect zinc availability in *S. aureus*. These results support the additional

https://doi.org/10.1021/jacs.1c02622
J. Am. Chem. Soc. 2021, 143, 12003−12013

mode of action of the hybrid antibiotic in reducing metal availability in a Gram-positive pathogen.

Having shown that thiomarinol maintains the modes of action of its constituents, we examined the interactions between DTP and pseudomonic acids A or C (mupirocin or PAC) in combination for potential synergistic effects. Interestingly, checkerboard assays against MRSA COL reveals an additive relationship for the combination of mupirocin and holomycin as well as that of PAC and holomycin (Figure S24). A concentration of 0.25 μM PAC or mupirocin in combination with 0.3 μM holomycin is required to fully inhibit growth of MRSA COL; thus, both combinations are approximately 100-fold less potent than the hybrids PAC-holo and thiomarinol (MICs of 0.002 μM). These data reveal that the covalent linkage to the DTP is required to significantly potentiate the antibiotic activity of mupirocin or PAC against MRSA.

We investigated the development of thiomarinol resistance by culturing MRSA COL in the presence of increasing concentrations of thiomarinol using the same protocol that was used to generate ^{LL}MR mutants[38] (Figure S25). These strains are 5−10-fold more resistant to thiomarinol and 12.5−25-fold more resistant to mupirocin than wild type MRSA COL (Table 1). The increase in resistance is modest compared to the 400-fold increase in MIC to mupirocin in the resistant mutants that were raised in the presence of mupirocin (^{LL}MR MRSA) under the same conditions. We looked for spontaneous mutations in IleRS in the thiomarinol-resistant strains and identified a G593D mutation in two strains and a P606S mutation in the third strain, which may contribute to thiomarinol resistance. While a Gly593 to Val mutation was reported in a ^{LL}MR MRSA mutant,[37,38] an IleRS mutation at Pro606 had not been observed. Thiomarinol remains highly effective against the G593D and P606S IleRS mutants (MICs of 0.02 and 0.01 μM).

DISCUSSION

We identified IleRS as a target for thiomarinol and its synthetic analogue, pseudomonyl C holothinamide (PAC-holo). Using a chemical genomics screen of an essential gene knockdown library in *B. subtilis*, we found that the *ileS* knockdown is the most sensitized to PAC-holo and mupirocin among the 242 essential genes analyzed; PAC-holo most strongly correlates with mupirocin among the 36 compounds tested. In agreement with our chemical genomics findings, the thiomarinol biosynthetic gene cluster contains an *ileS* homologue (*tmlM*) that likely provides self-resistance for the producing bacterium.[43] In addition, the chemical genomics screen indicates that the other DTPs—holomycin and thiolutin—and gliotoxin do not target IleRS. These compounds exhibit different chemical−gene interactions from PAC-holo and mupirocin: the *ileS* knockdown was insensitive, while knockdowns in *menA* (menaquinone biosynthesis) and *resC* (cytochrome biogenesis) were hypersensitive. Further, the disulfide-containing natural products, holomycin, thiolutin, and gliotoxin, exhibit the strongest correlations observed in this screen, corroborating the results from our previous chemical genomics screen that involved 3900 nonessential *E. coli* gene knockouts[18] and further suggesting these compounds exert a similar mode of action. This mode of action may involve inhibition of metabolic processes as suggested by the enrichment of metabolic genes (e.g., *menA* and *resC*) in the knockdowns hypersensitized to these disulfide-containing antibiotics.

We characterized inhibition of IleRS by thiomarinol using biochemical and biophysical methods. Thiomarinol potently inhibits IleRS with a K_i^{app} of 19 ± 4 nM under steady-state conditions, similar to that of 12 ± 2 nM for mupirocin. Combining the data obtained from ITC and CD thermal melt experiments allowed for the calculation of an estimated $K_{d,25\,°C}$ of 18 ± 7 pM for mupirocin binding to IleRS and an exceptionally low $K_{d,25\,°C}$ of 11 ± 6 fM for thiomarinol binding to IleRS, a 1600-fold higher affinity than mupirocin. The much lower K_d than K_i^{app} value could be due to the nature of bisubstrate inhibition as well as the sensitivity limit of the inhibition assay. Mupirocin is a bisubstrate inhibitor of IleRS and exhibits a competitive inhibitory mechanism with both substrates, L-Ile and ATP.[35] We expect that thiomarinol exhibits a mode of inhibition similar to that of mupirocin given the structural resemblance between the two antibiotics; therefore, the bisubstrate inhibition complicates the calculation of the true inhibition constant of thiomarinol, which is likely much lower than K_i^{app} and the estimated K_i for competition with a single substrate L-Ile. Additionally, the low picomolar sensitivity limit of the ATP-[^{32}P]PP$_i$ exchange inhibition assay cannot capture femtomolar potencies. Due to the competitive mechanism of inhibition, the K_d values we obtained using calorimetry and stability shift assays more likely reflect the actual potencies of mupirocin and thiomarinol, which are in the low picomolar and femtomolar range.

Notably, the synthetic hybrid PAC-holo complexed with IleRS displays a stability similar to that of mupirocin as determined by CD thermal melt experiments while the DTP holomycin does not inhibit or bind to IleRS. Together, the data indicate that the DTP makes no significant interactions with IleRS by itself or when linked with PAC. The marinolic acid A portion of thiomarinol A differs from mupirocin and PAC by alkyl chain length (*n* of 7, 8, and 8, respectively) and an additional hydroxyl at C-4 (R_1). These unique structural features may play a role in enhancing interactions between thiomarinol and IleRS at the active site. Although PAC-holo exhibits a weaker *in vitro* interaction with IleRS than the natural product thiomarinol, PAC-holo is equally effective as thiomarinol against MRSA in laboratory culture, hinting at the therapeutic potential of this natural product derivative. In summary, our results reveal that thiomarinol is one of the tightest IleRS binders to date, on par with the femtomolar binders obtained from an extensive medicinal chemistry campaign.[27] Our discovery highlights the potency and therapeutic potential of hybrid natural products and the derivatives thereof.

We demonstrated that thiomarinol remains effective against clinical MRSA strains that have acquired low-level or high-level mupirocin resistance (^{LL}MR or ^{HL}MR). Although the activity of thiomarinol is reduced by 40- and 250-fold against ^{LL}MR and ^{HL}MR MRSA, respectively, the potency of the hybrid is still higher than or comparable to the activity of mupirocin against sensitive MRSA. Compared to holomycin, which is equally active against mupirocin-sensitive, ^{LL}MR, and ^{HL}MR MRSA, thiomarinol is 3 orders of magnitude more active against mupirocin-sensitive MRSA and 10-fold more active against ^{HL}MR MRSA. Thus, the DTP portion of thiomarinol likely plays a more significant role in antimicrobial activity as the level of mupirocin-resistance increases in MRSA. Like holomycin and thiolutin,[18] the DTP of thiomarinol may also disrupt metal homeostasis in the bacterial cell, which may help thiomarinol overcome high-level mupirocin resistance. In

https://doi.org/10.1021/jacs.1c02622
J. Am. Chem. Soc. 2021, 143, 12003−12013

support of the metal chelation mechanism, we demonstrate that thiomarinol can chelate zinc *in vitro* and its inhibitory effect against MRSA involves the reduction of zinc availability. Additionally, both thiomarinol and PAC-holo inhibit zinc enzymes *in vitro*.[19] These data indicate that the zinc chelation properties of thiomarinol contribute to antibiotic activity. A dual mechanism has been described for the hybrid natural product everninomicin P that overcomes resistance to either of its constituents: a macrolide and octasaccharide; both components target the 70S ribosome and inhibit translation.[11] Our results suggest that the mupirocin and DTP constituents of thiomarinol likely enact two very different antimicrobial mechanisms—targeting translation by inhibiting IleRS and causing metal dysregulation by chelating metals, respectively—to overcome antibiotic resistance.

We found that MRSA could develop spontaneous thiomarinol resistance, but to a much lesser degree than mupirocin resistance during the same number of serial passages; the resulting MRSA mutants are only 5−10-fold more resistant to thiomarinol and remain sensitive to mupirocin. These data suggest that the hybridity of thiomarinol helps reduce the rise of resistance. We showed that the two antimicrobial components of thiomarinol and its synthetic analogue, PAC-holo, are additive in combination and must be covalently linked to significantly increase efficacy against mupirocin-sensitive MRSA. Increased cellular accumulation is a common mechanism to potentiate antibiotic efficacy that is used by the newly FDA-approved bifunctional antibiotic, cefiderocol,[5,6] which evades antibiotic resistance through increased compound uptake. PAC-holo-hypersensitive knockdowns are enriched with genes involved in peptidoglycan synthesis and cell shape regulation; this observation hints at a cell envelope target or increased cellular accumulation for PAC-holo that could contribute to the synergy of the hybrid molecule.[59,60] The mechanism by which hybridity potentiates the activity will be the focus of future studies.

CONCLUSION

Our work demonstrates that the hybrid antibiotic thiomarinol is a dual acting antibiotic: a potent inhibitor of IleRS and a metal chelator that reduces intracellular zinc availability. By conjugating an analogue of the IleRS-inhibiting antimicrobial mupirocin with a metal-chelating antibiotic, holothin, thiomarinol retains the ability to target IleRS but binds to IleRS significantly more tightly than mupirocin at femtomolar affinities. In comparison to mupirocin, thiomarinol exhibits higher potency against MRSA in culture and remains active against mupirocin-resistant MRSA at concentrations below cytotoxic levels. Additionally, a lower level of resistance develops in MRSA toward thiomarinol than toward mupirocin. We also investigated PAC-holo, a highly effective synthetic hybrid and thiomarinol derivative; we show that for both thiomarinol and PAC-holo covalent linkage between the antibiotic constituents is required for the high potency. The broad antimicrobial spectrum, low level of resistance, and activity against mupirocin-resistant isolates render thiomarinol a promising therapeutic lead and a potential model for hybrid antibiotics to overcome antimicrobial resistance.

ASSOCIATED CONTENT

Supporting Information

The Supporting Information is available free of charge at https://pubs.acs.org/doi/10.1021/jacs.1c02622.

Materials, methods, and supplemental figures (PDF)

Chemical genomics data including *B. subtilis* CRISPRi library information, chemical treatment conditions, chemical−gene scores, and GO analysis (XLSX)

AUTHOR INFORMATION

Corresponding Author

Bo Li − *Department of Chemistry, University of North Carolina at Chapel Hill, Chapel Hill, North Carolina 27599, United States; Department of Microbiology and Immunology, University of North Carolina at Chapel Hill, Chapel Hill, North Carolina 27599, United States;* orcid.org/0000-0002-8019-8891; Email: boli@email.unc.edu

Authors

Rachel A. Johnson − *Department of Chemistry, University of North Carolina at Chapel Hill, Chapel Hill, North Carolina 27599, United States;* orcid.org/0000-0003-1958-2218

Andrew N. Chan − *Department of Chemistry, University of North Carolina at Chapel Hill, Chapel Hill, North Carolina 27599, United States;* orcid.org/0000-0002-4257-7436

Ryan D. Ward − *Pharmaceutical Sciences Division, School of Pharmacy, University of Wisconsin-Madison, Madison, Wisconsin 53705, United States; Laboratory of Genetics, University of Wisconsin-Madison, Madison, Wisconsin 53706, United States*

Caylie A. McGlade − *Department of Chemistry, University of North Carolina at Chapel Hill, Chapel Hill, North Carolina 27599, United States*

Breanne M. Hatfield − *Department of Chemistry, University of North Carolina at Chapel Hill, Chapel Hill, North Carolina 27599, United States*

Jason M. Peters − *Pharmaceutical Sciences Division, School of Pharmacy, University of Wisconsin-Madison, Madison, Wisconsin 53705, United States; Great Lakes Bioenergy Research Center, Wisconsin Energy Institute, University of Wisconsin-Madison, Madison, Wisconsin 53726, United States*

Complete contact information is available at: https://pubs.acs.org/10.1021/jacs.1c02622

Author Contributions

#R.A.J. and A.N.C.: These authors contributed equally to this study

Notes

The authors declare no competing financial interest.

ACKNOWLEDGMENTS

The authors thank Walter Wever for making PAC-holo; Elissabetta Massolo, and Xiaoyan Chen (UNC Chapel Hill) for synthesizing holomycin; Carol Gross (UCSF), Gary Pielak, Charlie Carter, Tishan Williams, and Candice Crilly (UNC Chapel Hill), and Thomas Meek (Texas A&M) for helpful discussions; Joseph Turner (North Carolina State University) for assistance with MATLAB coding; Thomas Kehl-Fie (University of Illinois Urbana−Champaign) for MRSA Newman strains; Gerry Wright (McMaster University) for access to instrumentation for antibiotic testing in microplates; Ash Tripathy (UNC Macromolecular Interactions Facility) for assistance with ITC and CD thermal melt experiments; and Rachel M. Johnson for manuscript review. This work is supported by the National Institutes of Health

(DP2HD094657 to B.L.), the Packard Fellowship for Science and Engineering (B.L.), a Career Transition Award from the NIH National Institute of Allergy and Infectious Diseases (K22AI137122 to J.M.P.), and UNC Chapel Hill. R.D.W. was supported by the Predoctoral Training Program in Genetics (5T32GM007133-46). R.A.J. and B.M.H. acknowledge support from the Clare Boothe Luce Fellowship for Women in Science, and R.A.J. recognizes a Molecular and Cellular Biophysics Training Grant (T32GM008570).

REFERENCES

(1) World Health Organization. *2019 Antibacterial Agents in Clinical Development: An Analysis of the Antibacterial Clinical Development Pipeline*; World Health Organization: Geneva, 2019.
(2) Newman, D. J.; Cragg, G. M. Natural products as sources of new drugs over the nearly four decades from 01/1981 to 09/2019. *J. Nat. Prod.* **2020**, *83* (3), 770−803.
(3) Walsh, C. T.; Wencewicz, T. A. Prospects for new antibiotics: A molecule-centered perspective. *J. Antibiot.* **2014**, *67* (1), 7−22.
(4) Klahn, P.; Brönstrup, M. Bifunctional antimicrobial conjugates and hybrid antimicrobials. *Nat. Prod. Rep.* **2017**, *34* (7), 832−885.
(5) Wu, J. Y.; Srinivas, P.; Pogue, J. M. Cefiderocol: a novel agent for the management of multidrug-resistant Gram-negative organisms. *J. Infect. Dis. Ther.* **2020**, *9* (1), 17−40.
(6) Aoki, T.; Yoshizawa, H.; Yamawaki, K.; Yokoo, K.; Sato, J.; Hisakawa, S.; Hasegawa, Y.; Kusano, H.; Sano, M.; Sugimoto, H.; Nishitani, Y.; Sato, T.; Tsuji, M.; Nakamura, R.; Nishikawa, T.; Yamano, Y. Cefiderocol (S-649266), a new siderophore cephalosporin exhibiting potent activities against *Pseudomonas aeruginosa* and other gram-negative pathogens including multi-drug resistant bacteria: Structure activity relationship. *Eur. J. Med. Chem.* **2018**, *155*, 847−868.
(7) Schimana, J.; Fiedler, H. P.; Groth, I.; Sussmuth, R.; Beil, W.; Walker, M.; Zeeck, A. Simocyclinones, novel cytostatic angucyclinone antibiotics produced by *Streptomyces antibioticus* Tu 6040. I. Taxonomy, fermentation, isolation and biological activities. *J. Antibiot.* **2000**, *53* (8), 779−787.
(8) Holzenkampfer, M.; Walker, M.; Zeeck, A.; Schimana, J.; Fiedler, H. P. Simocyclinones, novel cytostatic angucyclinone antibiotics produced by *Streptomyces antibioticus* Tu 6040 II. Structure elucidation and biosynthesis. *J. Antibiot.* **2002**, *55* (3), 301−7.
(9) Edwards, M. J.; Flatman, R. H.; Mitchenall, L. A.; Stevenson, C. E. M.; Le, T. B. K.; Clarke, T. A.; McKay, A. R.; Fiedler, H. P.; Buttner, M. J.; Lawson, D. M.; Maxwell, A. A crystal structure of the bifunctional antibiotic simocyclinone D8, bound to DNA gyrase. *Science* **2009**, *326* (5958), 1415−1418.
(10) Chen, M.; Wang, R.; Zhao, W.; Yu, L.; Zhang, C.; Chang, S.; Li, Y.; Zhang, T.; Xing, J.; Gan, M.; Feng, F.; Si, S. Isocoumarindole A, a chlorinated isocoumarin and indole alkaloid hybrid metabolite from an endolichenic fungus *Aspergillus* sp. *Org. Lett.* **2019**, *21* (5), 1530−1533.
(11) Limbrick, E.; Graf, M.; Derewacz, D. K.; Nguyen, F.; Spraggins, J. M.; Wieland, M.; Ynigez-Gutierrez, A.; Reisman, B. J.; Zinshteyn, B.; McCulloch, K. M.; Iverson, T. M.; Green, R.; Wilson, D. N.; Bachmann, B. O. A bifunctional nitrone conjugated secondary metabolite targeting the ribosome. *J. Am. Chem. Soc.* **2020**, *142* (43), 18369−18377.
(12) Shiozawa, H.; Kagasaki, T.; Kinoshita, T.; Haruyama, H.; Domon, H.; Utsui, Y.; Kodama, K.; Takahashi, S. Thiomarinol, a new hybrid antimicrobial antibiotic produced by a marine bacterium: fermentation, isolation, structure, and antimicrobial activity. *J. Antibiot.* **1993**, *46* (12), 1834−1842.
(13) Shiozawa, H.; Kagasaki, T.; Torikata, A.; Tanaka, N.; Fujimoto, K.; Hata, T.; Furukawa, Y.; Takahashi, S. Thiomarinols B and C, new antimicrobial antibiotics produced by a marine bacterium. *J. Antibiot.* **1995**, *48* (8), 907−909.
(14) Shiozawa, H.; Shimada, A.; Takahashi, S. Thiomarinols D, E, F and G, new hybrid antimicrobial antibiotics produced by a marine bacterium; isolation, structure, and antimicrobial activity. *J. Antibiot.* **1997**, *50* (5), 449−452.
(15) Li, B.; Wever, W. J.; Walsh, C. T.; Bowers, A. A. Dithiolopyrrolones: biosynthesis, synthesis, and activity of a unique class of disulfide-containing antibiotics. *Nat. Prod. Rep.* **2014**, *31* (7), 905−23.
(16) Ettlinger, L.; Gäumann, E.; Hütter, R.; Keller-Schierlein, W.; Kradolfer, F.; Neipp, L.; Prelog, V.; Zähner, H. Stoffwechselprodukte von Actinomyceten 17. Mitteilung Holomycin. *Helv. Chim. Acta* **1959**, *42* (2), 563−569.
(17) Celmer, W. D.; Tanner, F. W.; Harfenist, M.; Lees, T. M.; Solomons, I. A. Characterization of the antibiotic thiolutin and its relationship with aureothricin. *J. Am. Chem. Soc.* **1952**, *74* (24), 6304−6305.
(18) Chan, A. N.; Shiver, A. L.; Wever, W. J.; Razvi, S. Z. A.; Traxler, M. F.; Li, B. Role for dithiolopyrrolones in disrupting bacterial metal homeostasis. *Proc. Natl. Acad. Sci. U. S. A.* **2017**, *114* (10), 2717−2722.
(19) Lauinger, L.; Li, J.; Shostak, A.; Cemel, I. A.; Ha, N.; Zhang, Y.; Merkl, P. E.; Obermeyer, S.; Stankovic-Valentin, N.; Schafmeier, T.; Wever, W. J.; Bowers, A. A.; Carter, K. P.; Palmer, A. E.; Tschochner, H.; Melchior, F.; Deshaies, R. J.; Brunner, M.; Diernfellner, A. Thiolutin is a zinc chelator that inhibits the Rpn11 and other JAMM metalloproteases. *Nat. Chem. Biol.* **2017**, *13* (7), 709−714.
(20) Sutherland, R.; Boon, R. J.; Griffin, K. E.; Masters, P. J.; Slocombe, B.; White, A. R. Antibacterial activity of mupirocin (pseudomonic acid), a new antibiotic for topical use. *Antimicrob. Agents Chemother.* **1985**, *27* (4), 495−498.
(21) CDC. *Antibiotic Resistant Threats in the United States, 2019*; U.S. Department of Health and Human Services, CDC: Atlanta, GA, 2019; pp 1−138.
(22) Chain, E. B.; Mellows, G. Pseudomonic acid. Part 3. Structure of pseudomonic acid B. *J. Chem. Soc., Perkin Trans. 1* **1977**, *3*, 318−322.
(23) Clayton, J. P.; O'Hanlon, P. J.; Rogers, N. H. The structure and configuration of pseudomonic acid C. *Tetrahedron Lett.* **1980**, *21* (9), 881−884.
(24) Wang, L.; Song, Z.; Race, P. R.; Spencer, J.; Simpson, T. J.; Crump, M. P.; Willis, C. L. Mixing and matching genes of marine and terrestrial origin in the biosynthesis of the mupirocin antibiotics. *Chem. Sci.* **2020**, *11* (20), 5221−5226.
(25) Hughes, J.; Mellows, G. Inhibition of isoleucyl-transfer ribonucleic acid synthetase in *Escherichia coli* by pseudomonic acid. *Biochem. J.* **1978**, *176* (1), 305−18.
(26) Hughes, J.; Mellows, G. On the mode of action of pseudomonic acid: Inhibition of protein synthesis in *Staphylococcus aureus*. *J. Antibiot.* **1978**, *31* (4), 330−335.
(27) Brown, M. J.; Mensah, L. M.; Doyle, M. L.; Broom, N. J.; Osbourne, N.; Forrest, A. K.; Richardson, C. M.; O'Hanlon, P. J.; Pope, A. J. Rational design of femtomolar inhibitors of isoleucyl tRNA synthetase from a binding model for pseudomonic acid A. *Biochemistry* **2000**, *39* (20), 6003−6011.
(28) Pope, A. J.; Moore, K. J.; McVey, M.; Mensah, L.; Benson, N.; Osbourne, N.; Broom, N.; Brown, M. J.; O'Hanlon, P. Characterization of isoleucyl-tRNA synthetase from *Staphylococcus aureus*. II. Mechanism of inhibition by reaction intermediate and pseudomonic acid analogues studied using transient and steady-state kinetics. *J. Biol. Chem.* **1998**, *273* (48), 31691−31701.
(29) Francklyn, C. S.; Mullen, P. Progress and challenges in aminoacyl-tRNA synthetase-based therapeutics. *J. Biol. Chem.* **2019**, *294* (14), 5365−5385.
(30) Pope, A. J.; Lapointe, J.; Mensah, L.; Benson, N.; Brown, M. J.; Moore, K. J. Characterization of isoleucyl-tRNA synthetase from *Staphylococcus aureus*. I: Kinetic mechanism of the substrate activation reaction studied by transient and steady-state techniques. *J. Biol. Chem.* **1998**, *273* (48), 31680−31690.
(31) Hurdle, J. G.; O'Neill, A. J.; Chopra, I. Prospects for aminoacyl-tRNA synthetase inhibitors as new antimicrobial agents. *Antimicrob. Agents Chemother.* **2005**, *49* (12), 4821−4833.

https://doi.org/10.1021/jacs.1c02622
J. Am. Chem. Soc. 2021, 143, 12003−12013

(32) Hughes, J.; Mellows, G. Interaction of pseudomonic acid A with *Escherichia coli* B isoleucyl-tRNA synthetase. *Biochem. J.* **1980**, *191* (1), 209−219.
(33) Chung, S.; Kim, S.; Ryu, S. H.; Hwang, K. Y.; Cho, Y. Structural basis for the antibiotic resistance of eukaryotic isoleucyl-tRNA synthetase. *Mol. Cells* **2020**, *43* (4), 350−359.
(34) Williams, T. L.; Yin, Y. H. W.; Carter, C. W. Selective inhibition of bacterial tryptophanyl-tRNA synthetases by indolmycin is mechanism-based. *J. Biol. Chem.* **2016**, *291* (1), 255−265.
(35) Nakama, T.; Nureki, O.; Yokoyama, S. Structural basis for the recognition of isoleucyl-adenylate and an antibiotic, mupirocin, by isoleucyl-tRNA synthetase. *J. Biol. Chem.* **2001**, *276* (50), 47387−47393.
(36) Silvian, L. F.; Wang, J.; Steitz, T. A. Insights into editing from an Ile-tRNA synthetase structure with tRNAIle and mupirocin. *Science* **1999**, *285* (5430), 1074−1077.
(37) Lee, A. S.; Gizard, Y.; Empel, J.; Bonetti, E. J.; Harbarth, S.; Francois, P. Mupirocin-induced mutations in *ileS* in various genetic backgrounds of methicillin-resistant *Staphylococcus aureus*. *J. Clin. Microbiol.* **2014**, *52* (10), 3749−3754.
(38) Thomas, D. G.; Wilson, J. M.; Day, M. J.; Russell, A. D. Mupirocin resistance in staphylococci: development and transfer of isoleucyl-tRNA synthetase-mediated resistance *in vitro*. *J. Appl. Microbiol.* **1999**, *86* (4), 715−722.
(39) Seah, C.; Alexander, D. C.; Louie, L.; Simor, A.; Low, D. E.; Longtin, J.; Melano, R. G. MupB, a new high-level mupirocin resistance mechanism in *Staphylococcus aureus*. *Antimicrob. Agents Chemother.* **2012**, *56* (4), 1916−1920.
(40) Hodgson, J. E.; Curnock, S. P.; Dyke, K. G.; Morris, R.; Sylvester, D. R.; Gross, M. S. Molecular characterization of the gene encoding high-level mupirocin resistance in *Staphylococcus aureus* J2870. *Antimicrob. Agents Chemother.* **1994**, *38* (5), 1205−1208.
(41) Ramsey, M. A.; Bradley, S. F.; Kauffman, C. A.; Morton, T. M. Identification of chromosomal location of *mupA* gene, encoding low-level mupirocin resistance in staphylococcal isolates. *Antimicrob. Agents Chemother.* **1996**, *40* (12), 2820−2823.
(42) Park, S. Y.; Kim, S. M.; Park, S. D. The prevalence, genotype and antimicrobial susceptibility of high- and low-level mupirocin resistant methicillin-resistant *Staphylococcus aureus*. *Ann. Dermatol.* **2012**, *24* (1), 32−38.
(43) Fukuda, D.; Haines, A. S.; Song, Z.; Murphy, A. C.; Hothersall, J.; Stephens, E. R.; Gurney, R.; Cox, R. J.; Crosby, J.; Willis, C. L.; Simpson, T. J.; Thomas, C. M. A natural plasmid uniquely encodes two biosynthetic pathways creating a potent anti-MRSA antibiotic. *PLoS One* **2011**, *6* (3), e18031−e18031.
(44) Timmermans, M. L.; Picott, K. J.; Ucciferri, L.; Ross, A. C. Culturing marine bacteria from the genus *Pseudoalteromonas* on a cotton scaffold alters secondary metabolite production. *MicrobiologyOpen* **2019**, *8* (5), No. e00724.
(45) Chan, A. N.; Wever, W. J.; Massolo, E.; Allen, S. E.; Li, B. Reducing holomycin thiosulfonate to its disulfide with thiols. *Chem. Res. Toxicol.* **2019**, *32* (3), 400−404.
(46) Maansson, M.; Vynne, N. G.; Klitgaard, A.; Nybo, J. L.; Melchiorsen, J.; Nguyen, D. D.; Sanchez, L. M.; Ziemert, N.; Dorrestein, P. C.; Andersen, M. R.; Gram, L. An integrated metabolomic and genomic mining workflow to uncover the biosynthetic potential of bacteria. *mSystems* **2016**, *1* (3), e00028-15.
(47) Dunn, Z. D.; Wever, W. J.; Economou, N. J.; Bowers, A. A.; Li, B. Enzymatic basis of "hybridity" in thiomarinol biosynthesis. *Angew. Chem. Int. Ed.* **2015**, *54* (17), 5137−5141.
(48) Kohanski, M. A.; Dwyer, D. J.; Collins, J. J. How antibiotics kill bacteria: From targets to networks. *Nat. Rev. Microbiol.* **2010**, *8* (6), 423−435.
(49) Peters, J. M.; Colavin, A.; Shi, H.; Czarny, T. L.; Larson, M. H.; Wong, S.; Hawkins, J. S.; Lu, C. H. S.; Koo, B. M.; Marta, E.; Shiver, A. L.; Whitehead, E. H.; Weissman, J. S.; Brown, E. D.; Qi, L. S.; Huang, K. C.; Gross, C. A. A comprehensive, CRISPR-based functional analysis of essential genes in bacteria. *Cell* **2016**, *165* (6), 1493−1506.
(50) Koo, B.-M.; Kritikos, G.; Farelli, J. D.; Todor, H.; Tong, K.; Kimsey, H.; Wapinski, I.; Galardini, M.; Cabal, A.; Peters, J. M.; Hachmann, A.-B.; Rudner, D. Z.; Allen, K. N.; Typas, A.; Gross, C. A. Construction and analysis of two genome-scale deletion libraries for *Bacillus subtilis*. *Cell Syst.* **2017**, *4* (3), 291−305.
(51) Bernardo, P. H.; Brasch, N.; Chai, C. L.; Waring, P. A novel redox mechanism for the glutathione-dependent reversible uptake of a fungal toxin in cells. *J. Biol. Chem.* **2003**, *278* (47), 46549−55.
(52) Collins, S. R.; Schuldiner, M.; Krogan, N. J.; Weissman, J. S. A strategy for extracting and analyzing large-scale quantitative epistatic interaction data. *Genome Biol.* **2006**, *7*, R63.
(53) Fersht, A. R.; Ashford, J. S.; Bruton, C. J.; Jakes, R.; Koch, G. L.; Hartley, B. S. Active site titration and aminoacyl adenylate binding stoichiometry of aminoacyl-tRNA synthetases. *Biochemistry* **1975**, *14* (1), 1−4.
(54) Copeland, R. A. Tight binding inhibition. In*Evaluation of Enzyme Inhibitors in Drug Discovery*; John Wiley & Sons, Inc.: 2013; pp 245−285.
(55) Brandts, J. F.; Lin, L.-N. Study of strong to ultralight protein interactions using differential scanning calorimetry. *Biochemistry* **1990**, *29* (29), 6927−6940.
(56) Hurdle, J. G.; O'Neill, A. J.; Ingham, E.; Fishwick, C.; Chopra, I. Analysis of mupirocin resistance and fitness in *Staphylococcus aureus* by molecular genetic and structural modeling techniques. *Antimicrob. Agents Chemother.* **2004**, *48* (11), 4366−76.
(57) Diep, B. A.; Gill, S. R.; Chang, R. F.; Phan, T. H.; Chen, J. H.; Davidson, M. G.; Lin, F.; Lin, J.; Carleton, H. A.; Mongodin, E. F.; Sensabaugh, G. F.; Perdreau-Remington, F. Complete genome sequence of USA300, an epidemic clone of community-acquired methicillin-resistant *Staphylococcus aureus*. *Lancet* **2006**, *367* (9512), 731−739.
(58) Grim, K. P.; San Francisco, B.; Radin, J. N.; Brazel, E. B.; Kelliher, J. L.; Párraga Solórzano, P. K.; Kim, P. C.; McDevitt, C. A.; Kehl-Fie, T. E. The metallophore staphylopine enables *Staphylococcus aureus* to compete with the host for zinc and overcome nutritional immunity. *mBio* **2017**, *8* (5), e01281-17.
(59) Ontong, J. C.; Ozioma, N. F.; Voravuthikunchai, S. P.; Chusri, S. Synergistic antibacterial effects of colistin in combination with aminoglycoside, carbapenems, cephalosporins, fluoroquinolones, tetracyclines, fosfomycin, and piperacillin on multidrug resistant *Klebsiella pneumoniae* isolates. *PLoS One* **2021**, *16* (1), No. e0244673.
(60) Bergen, P. J.; Smith, N. M.; Bedard, T. B.; Bulman, Z. P.; Cha, R.; Tsuji, B. T. Rational combinations of polymyxins with other antibiotics. In*Advances in Experimental Medicine and Biology*; Li, J., Nation, R., Kaye, K., Eds.; Springer International Publishing: 2019; Vol. *1145*, pp 251−288.

https://doi.org/10.1021/jacs.1c02622
J. Am. Chem. Soc. 2021, 143, 12003−12013